Exotic molecules consisting of an antiproton and a hydrogen atom

Kazuhiro Sakimoto
Institute of Space and Astronautical Science, Japan Aerospace Exploration Agency, Yoshinodai 3-1-1, Chuo-ku, Sagamihara, Kanagawa 252-5210, Japan

(Received 8 July 2018; published 8 October 2018)

A theoretical study is conducted on the stability of exotic antiproton-hydrogen molecular anions ($\bar{p}$H), which in the separated atom limit correlate with $\bar{p} + \mathrm{H}(n = 2)$ (n being the principal quantum number). The $\bar{p}$H molecule in the electronic ground state is highly unstable due to pair annihilation and autodetachment ($\rightarrow \bar{p}p + e$). However, if the $\bar{p}$H molecule is electronically excited, the molecular stability can be drastically improved. Since the excited states of the H atom have accidental degeneracy, the asymptotic form of the Born-Oppenheimer potential curve of $\bar{p} + \mathrm{H}(n = 2)$ behaves as $1/R^2$ (R being the relative distance), which can play a critical role in the bonding and stability of the molecule. It is found that the $\bar{p}$H molecule in the first electronic excited state and in a high rotational state is sufficiently stable and has a lifetime dominated by spontaneous radiative emission ($\rightarrow \bar{p} + \mathrm{H} + h\nu$). The $\bar{p}$H system is dynamically similar to H_2^-, which had been commonly considered to be unstable due to autodetachment. However, recent measurements of ion-beam sputtering unambiguously verified the existence of long-lived H_2^- molecules in high rotational states. This suggests that the $\bar{p}$H molecules may actually be created if one employs experimental means such as the chemical sputtering of hydrogen-rich targets with $\bar{p}$ beams.

DOI: 10.1103/PhysRevA.98.042503

I. INTRODUCTION

The exotic system, in which particles and antiparticles are bound together by atomic or molecular interaction, is of interest for the purpose of not merely producing it but also gaining a deep insight into the physics of antimatter in matter. The simplest and most fundamental examples of such exotic combinations are positronium $\mathrm{Ps} = ee^+$ (e^+ being a positron), protonium $\mathrm{Pn} = \bar{p}p$ ($\bar{p}$ being an antiproton), true muonium $\mu^-\mu^+$ ($\mu^\pm$ being a muon), and so on. These kinds of exotic two-body atoms (usually named by adding the suffix "-onium"), in which a particle and its antiparticle are bound by the attractive Coulomb interaction, have a decay channel attributable to pair annihilation. However, the rate of the pair annihilation decreases rapidly as the angular momentum of the atomic orbital becomes higher [1–3]. Therefore, the particle-antiparticle atoms in high angular momentum states can have long lifetimes. A variety of investigations have been done, particularly for the Ps atom [4,5]. Recent experimental studies further demonstrated the existence of positronium ions Ps^- [6] and also so-called di-positronium Ps_2 (also known as positronium molecules) [7]. Another notable example of the exotic system is an antiprotonic atom [8], in which the attractive Coulomb interaction between the antiproton and the atomic nucleus plays an important role in the bonding. Of particular interest is antiprotonic helium $\bar{p}\mathrm{He}^+$ [9–11]. In high-resolution spectroscopic studies of the $\bar{p}\mathrm{He}^+$ atom, the mass and electric charge of the antiproton can be precisely compared with the proton values [10–12]. Also for the $\bar{p}\mathrm{He}^+$ atom, the annihilation is negligible if the $\bar{p}$-He^+ orbital has a high angular momentum. This three-body system is composed of one electron and two heavy particles. An interesting finding is that the Born-Oppenheimer (BO) approximation is appropriate for describing the high angular momentum states of $\bar{p}\mathrm{He}^+$ [9,13]. In this sense, this exotic system shows a similarity to molecules (and is sometimes called an "atomcule"). It should be noted, however, that an Auger channel is open in this system, i.e., $\bar{p}\mathrm{He}^+ \rightarrow \bar{p}\mathrm{He}^{2+} + e$. Accordingly, one of the important subjects in the $\bar{p}\mathrm{He}^+$ study is to discuss the stability against the Auger decay [9–11].

Recently, there has been a great deal of progress in experiments producing antihydrogen $\bar{\mathrm{H}} = e^+\bar{p}$ at very low temperatures (~10 K) [14–16]. A lively concern is entertained for the $\bar{\mathrm{H}} + \mathrm{H}$ system: it has an attractive dispersion interaction asymptotically, and the BO approximation is appropriate at least for intermediate and large separations [17–24]. An interesting question to be posed is whether the $\bar{\mathrm{H}}\mathrm{H}$ system can exist as a molecule. Zygelman *et al.* [19] suggested that the $\bar{\mathrm{H}}\mathrm{H}$ molecule could be produced by radiative association in low-temperature conditions. However, this system has a decay channel of exoergic rearrangement reaction $\bar{\mathrm{H}}\mathrm{H} \rightarrow \bar{p}p + ee^+$ in addition to pair annihilation. Unfortunately, the $\bar{\mathrm{H}}\mathrm{H}$ molecule was found to be always highly unstable due to the rapid rearrangement decay [19,22–24]. As a similar subject, the stability of $\bar{p}$H molecular anions was examined [25]. Also in the $\bar{p} + \mathrm{H}$ system, the BO approximation works accurately except at small distances [26–30], and the polarization interaction, which has a range much longer than the dispersion interaction, was expected to be favorable for the bonding. However, the $\bar{p}$H molecule was again found to be unstable due to electron detachment $\bar{p}\mathrm{H} \rightarrow \bar{p}p + e$ [25]. The same conclusion can be drawn also for the stability of the charge conjugation system $p\bar{\mathrm{H}}$.

The $\bar{p}$H system considered in Ref. [25] was assumed to be in the electronic ground state. If the H atom is electronically excited, the BO potential of $\bar{p} + \mathrm{H}$ can have asymptotically a long-range term proportional to $1/R^2$, with R being the

relative distance [29,31,32]. This is because the H atom has a peculiarity of the degenerate sublevels with the same principal quantum number n [33]. (The nonrelativistic quantum mechanics is assumed for atomic processes.) The presence of the long-range potential $\propto 1/R^2$ was found to drastically influence the collision processes in $\bar{p} + \mathrm{H}(n = 2)$ at very low energies [32]. One can further expect that this long-range potential utterly alters the situation regarding the bonding of $\bar{p}$H.

The purpose of the present paper is to discuss the possibility of the existence of vibrational bound states of the exotic $\bar{p}$H molecule, which correlates with $\bar{p} + \mathrm{H}(n = 2)$ in the separated atom limit ($R \to \infty$). The paper is organized as follows. Section II provides some properties of the $\bar{p}$H system obtained within the framework of the BO approximation. If the $\bar{p}$H molecules were formed, the following decay processes could be important:

$$\bar{p}\mathrm{H} \to \text{(pair annihilation)} \tag{1}$$

$$\to \bar{p}\,p + e \text{ (autodetachment)} \tag{2}$$

$$\to \bar{p} + \mathrm{H}(1s) \text{ (predissociation)} \tag{3}$$

$$\to \bar{p} + \mathrm{H}(1s) + h\nu \text{ (spontaneous radiation).} \tag{4}$$

Of these, the annihilation is negligible for high rotational states of the $\bar{p}$H molecule. The BO approximation becomes meaningless at small R, where the electron detachment occurs immediately [30]. The autodetachment would be the most central decay channel. A preliminary discussion on the stability against the autodetachment is given in Sec. III. Nonadiabatic coupling causes the transition into the electronic ground state, though it would be insignificant. This transition appears as predissociation because the energy of $\bar{p}\mathrm{H}(n = 2)$ is higher than the dissociation limit of $\bar{p} + \mathrm{H}(1s)$. In the present case, the spontaneous radiative emission always leads to the dissociation $\bar{p} + \mathrm{H}(1s)$. To make a quantitative evaluation of the molecular stability, Sec. IV provides perturbation treatments for the atomic processes of Eqs. (2), (3) and (4). Section V presents the results of the calculations. The $\bar{p}$H system, to be considered as a sufficiently stable molecule, must have a lifetime that is comparable to the natural lifetime determined by the spontaneous radiation. Comparative discussions of H_2^+ and H_2^- molecules are presented in Sec. VI. Finally, Sec. VII gives further discussion.

II. BORN-OPPENHEIMER APPROXIMATION

The Hamiltonian of the whole system ($\bar{p}$-p-e) is written as

$$H = -\frac{1}{2\mu}\frac{\partial^2}{\partial \mathbf{R}^2} - \frac{1}{R} + H_{\mathrm{BO}}, \tag{5}$$

where $\mathbf{R}$ represents the position vector between $\bar{p}$ and p, and μ is the reduced mass of $\bar{p} + \mathrm{H}$. Here and in the following, atomic units are used unless otherwise stated. The electron mass is assumed to be negligible compared with the proton mass. The Hamiltonian H_{BO} is associated with the BO electronic state, i.e.,

$$H_{\mathrm{BO}} = -\frac{1}{2}\frac{\partial^2}{\partial \mathbf{r}^2} - \frac{1}{r} + \frac{1}{|\mathbf{R} - \mathbf{r}|}, \tag{6}$$

where $\mathbf{r}$ is the electron position vector. Introducing the body-fixed frame, in which the z axis is chosen along $\hat{\mathbf{R}}$, one can obtain the BO wave function $\chi_{n_1 n_2 \lambda}(R;\mathbf{r})$ and the adiabatic electron energy $\Lambda_{n_1 n_2 \lambda}(R)$ from the following Schrödinger equation:

$$H_{\mathrm{BO}}\,\chi_{n_1 n_2 \lambda}(R;\mathbf{r}) = \Lambda_{n_1 n_2 \lambda}(R)\,\chi_{n_1 n_2 \lambda}(R;\mathbf{r}), \tag{7}$$

with the normalization

$$\langle \chi_{n_1' n_2' \lambda'} | \chi_{n_1 n_2 \lambda} \rangle_{\mathbf{r}} = \delta_{n_1' n_1}\delta_{n_2' n_2}\delta_{\lambda' \lambda}, \tag{8}$$

where $\langle\ |\ \rangle_{\mathbf{r}}$ indicates the integration over the coordinates $\mathbf{r}$. The BO potential is given by

$$V_{n_1 n_2 \lambda}(R) = \Lambda_{n_1 n_2 \lambda}(R) - \frac{1}{R}. \tag{9}$$

Equation (7) is fully separable in prolate spheroidal coordinates [29]. The quantum numbers (n_1, n_2) are the numbers of nodes in the separated wave functions, and λ is the magnetic quantum number around $\hat{\mathbf{R}}$. In the separated atom limit ($R \to \infty$), the electron energy becomes $\Lambda_{n_1 n_2 \lambda}(\infty) = -1/(2n^2)$, with $n = n_1 + n_2 + |\lambda| + 1$ being the principal quantum number of the H atom. At large R, the quantum numbers (n_1, n_2, λ) are just identical to those introduced in the Stark effect [33,34]. The adiabatic electron energy $\Lambda_{n_1 n_2 \lambda}(R)$ was accurately calculated and tabulated by Wallis *et al.* [29]. The present notation (n_1, n_2, λ) corresponds to "(n_λ, n_μ, m)" defined by Wallis *et al.* [29].

Figure 1 shows the adiabatic electron energies $\Lambda_{n_1 n_2 \lambda}(R)$ for $n = 1$ and 2 [29] and the BO potentials $V_{n_1 n_2 \lambda}(R)$ for $n = 2$. In the $\bar{p} + \mathrm{H}$ system, there exists a critical distance $A_{n_1 n_2 \lambda}$ such that the electron energy is $\Lambda_{n_1 n_2 \lambda}(R) < 0$ only at $R > A_{n_1 n_2 \lambda}$. For the $(n_1, n_2, \lambda) = (0, 0, 0)$ state, which correlates with $\bar{p} + \mathrm{H}(1s)$ in the separated atom limit, $A_{n_1 n_2 \lambda}$ is especially known as the Fermi-Teller distance $R_{\mathrm{FT}} = 0.639$ a.u. [26–28]. If $n_2 = \lambda = 0$, the critical distance $A_{n_1 n_2 \lambda}$ is equal to $R_{\mathrm{FT}} = 0.639$ a.u. for any n_1 [35,36]. Coulson *et al.* [35] and Crawford [36] presented the critical distances also for other states, e.g., $A_{n_1, n_2 = 1, \lambda = 0} = 7.55$ a.u. and $A_{n_1, n_2 = 0, \lambda = \pm 1} = 3.79$ a.u. Of particular note is that the BO approximation completely fails at $R \leqslant A_{n_1 n_2 \lambda}$.

For the electronic ground state $(n_1, n_2, \lambda) = (0, 0, 0)$, the long-range part of the BO potential has the form $-\alpha/(2R^4)$, with $\alpha = -4.5$ a.u. being the polarizability of the H($1s$) atom. If the H atom is in an excited state, the BO potential can have a long-range term much slower than $1/R^4$. As $R \to \infty$, the BO potential generally becomes [31,32]

$$V_{n_1 n_2 \lambda}(R) \xrightarrow[R \to \infty]{} \frac{3n(n_2 - n_1)}{2R^2} - \frac{1}{2n^2}. \tag{10}$$

The BO potential at large R has an attractive long-range term $\propto -1/R^2$ for the electronic state with $n_1 > n_2$ and a repulsive term for $n_1 < n_2$; such long-range terms are missing for $n_1 = n_2$, as seen in Fig. 1. For the BO potential, which is asymptotically attractive, the vibrational bound motion may be realized. If the BO approximation is valid over the whole range of distances related to the vibrational motion, the vibrational state is given by solving

$$\left[-\frac{1}{2\mu}\frac{d^2}{dR^2} + V_{\mathrm{eff}}(R) + \frac{1}{2n^2}\right] F_{\mathrm{BO}}(R) = E_{\mathrm{BO}} F_{\mathrm{BO}}(R), \tag{11}$$

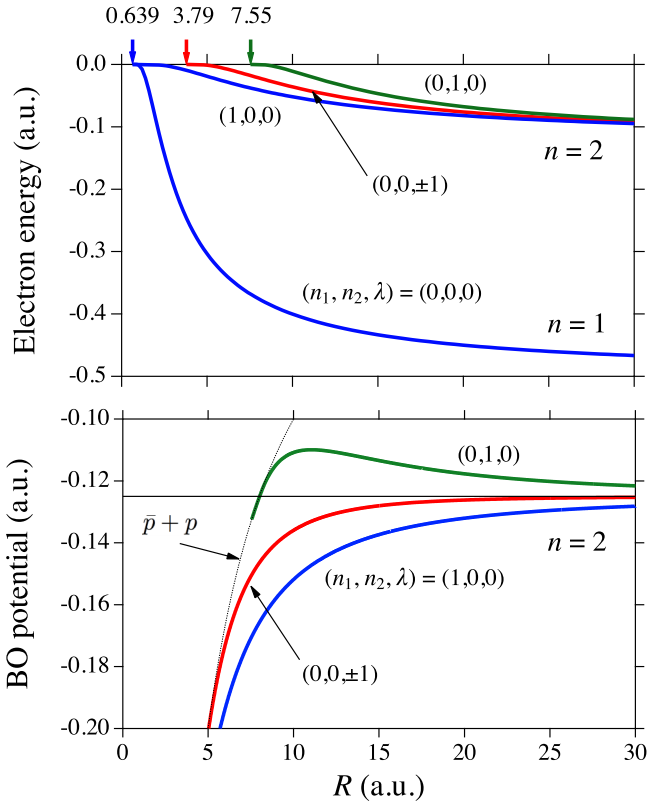

FIG. 1. Adiabatic electron energies $\Lambda_{n_1n_2\lambda}(R)$ and BO potentials $V_{n_1n_2\lambda}(R)$ of $\bar{p}+\mathrm{H}$, taken from Ref. [29]. The critical distances are $A_{n_1n_2\lambda} = R_{\mathrm{FT}} = 0.639$ a.u. for $(n_1, n_2, \lambda) = (0, 0, 0)$ and (1,0,0); $A_{n_1n_2\lambda} = 3.79$ a.u. for $(0, 0, \pm1)$; and $A_{n_1n_2\lambda} = 7.55$ a.u. for (0,1,0) [35,36]. In the lower figure, also plotted is the $\bar{p}+p$ potential curve (i.e., $-1/R$), which intersects with $V_{n_1n_2\lambda}(R)$ at $R = A_{n_1n_2\lambda}$.

where

$$V_{\mathrm{eff}}(R) = \frac{J(J+1)}{2\mu R^2} + V_{n_1n_2\lambda}(R) \tag{12}$$

is the effective potential, with J being the total angular momentum quantum number, $R^{-1}F_{\mathrm{BO}}(R)$ is the vibrational wave function, and E_{BO} is the vibrational energy relative to the dissociation limit of $\bar{p}+\mathrm{H}(n)$. Unfortunately, Eq. (11) lacks meaning at $R < A_{n_1n_2\lambda}$. For very high J, however, the relative motion is always limited to the outer region $R \gg A_{n_1n_2\lambda}$, due to the centrifugal potential $J(J+1)/(2\mu R^2)$. Therefore, Eq. (11) is reasonably good for describing the vibrational state if the system has a sufficiently high angular momentum J.

The $n = 2$ states consist of three kinds of sublevels $(n_1, n_2, \lambda) = (1, 0, 0)$, (0,1,0), and $(0, 0, \pm1)$. Of these, only the first electronic excited state (1,0,0) has the attractive term $\propto -1/R^2$, and the asymptotic form of its effective potential becomes

$$V_{\mathrm{eff}}(R) \xrightarrow[R\to\infty]{} \frac{J(J+1)-6\mu}{2\mu R^2} - \frac{1}{8}. \tag{13}$$

The term $\propto 1/R^2$ in Eq. (13) remains attractive if $J(J+1) < 6\mu$. This condition gives $J \leqslant J_{\max} = 73$, which is extremely higher than those ($J \lesssim 30$) related to the (0,0,0) state (Figs. 2 and 3). For the (1,0,0) state, it turns out that the effective potential with very high J can support vibrational states.

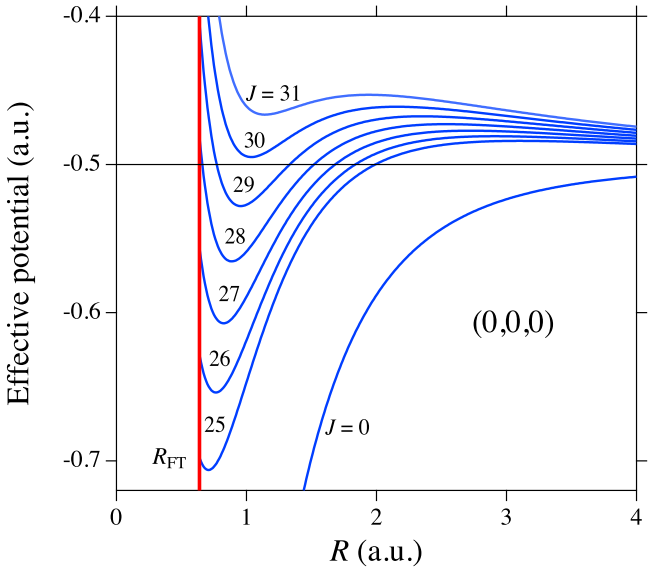

FIG. 2. Effective potentials $V_{\mathrm{eff}}(R) = J(J+1)/(2\mu R^2) + V_{n_1n_2\lambda}(R)$ of $\bar{p}+\mathrm{H}$ in the electronic ground state $(n_1, n_2, \lambda) = (0, 0, 0)$ for $J = 0$ and 25–31. The horizontal line indicates the $\mathrm{H}(n = 1)$ energy $-1/2$ a.u. The vertical line indicates the position of $R_{\mathrm{FT}} = 0.639$ a.u.

From another standpoint, as $R \to \infty$, the centrifugal and intermolecular interactions in Eq. (5) can be expressed by

$$\frac{\mathbf{L}^2 + 2\mu\hat{\mathbf{R}}\cdot\mathbf{r}}{2\mu R^2}, \tag{14}$$

where $\mathbf{L}$ is the orbital angular momentum operator of $\bar{p}+\mathrm{H}$. Diagonalizing the numerator with use of the degenerate (same n) states of the H atom gives the effective

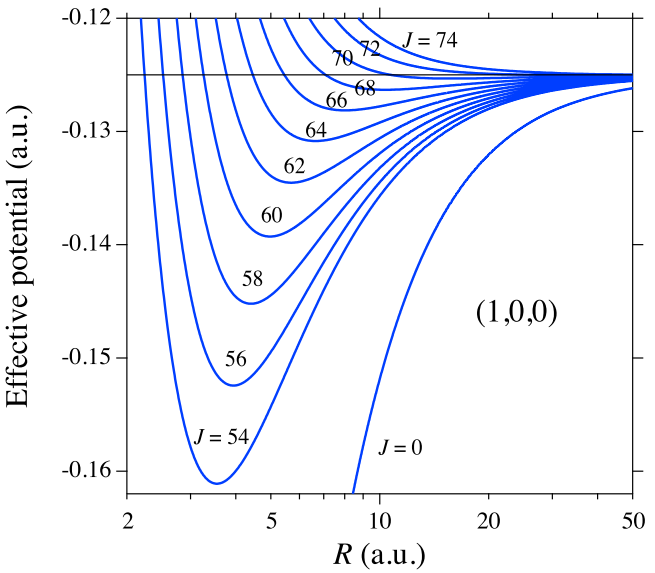

FIG. 3. Effective potentials $V_{\mathrm{eff}}(R) = J(J+1)/(2\mu R^2) + V_{n_1n_2\lambda}(R)$ of $\bar{p}+\mathrm{H}$ in the first electronic excited state $(n_1, n_2, \lambda) = (1, 0, 0)$ for $J = 0$ and 54–74. (Only an even number of J is considered.) The horizontal line indicates the $\mathrm{H}(n = 2)$ energy $-1/8$ a.u. The critical distance is $A_{100} = R_{\mathrm{FT}}$, but is not shown in the figure.

potential [31,37],

$$V_{\rm eff}(R) \xrightarrow[R\to\infty]{} \frac{\Omega}{2\mu R^2} - \frac{1}{2n^2}, \tag{15}$$

where Ω is the eigenvalue of the numerator in Eq. (14). The lowest eigenvalue for $n = 2$ [31,37], corresponding to the (1,0,0) state, is

$$\Omega = J^2 + J + 1 - \sqrt{(6\mu)^2 + (2J+1)^2}. \tag{16}$$

The condition $\Omega < 0$ gives $J \leqslant 73$, which is the same as the one obtained from Eq. (13). In the case of $\mu \gg J \gg 1$, indeed Ω becomes identical to the numerator of Eq. (13).

As in the case of the Coulomb potential, the long-range tail $\Omega/(2\mu R^2)$ with $\Omega < 0$ in $V_{\rm eff}(R)$ supports an infinite number of bound states. This can be directly verified by using the Bohr-Sommerfeld quantization rule:

$$\int_{R_1}^{R_2} p(R)\, dR = \left(v + \frac{1}{2}\right)\pi, \tag{17}$$

where

$$p(R) = \sqrt{2\mu\left[E_{\rm BO} - \frac{1}{2n^2} - V_{\rm eff}(R)\right]}, \tag{18}$$

R_1 (or R_2) is the inner (or outer) classical turning point, and v is the vibrational quantum number. In the case in which the vibrational energy is $E_{\rm BO} \sim 0$, there exists the region $R_{\rm dip} \leqslant R \leqslant R_2$, where $V_{\rm eff}(R)$ can be expressed by Eq. (15). In the limit of $E_{\rm BO} \to 0$, it is easy to show that Eq. (17) becomes ∞ (i.e., $v \to \infty$) and offers

$$E_{\rm BO} = -\exp\left[-\frac{2(v - v_0)\pi}{|\Omega|}\right], \tag{19}$$

where v_0 is the adjustment parameter coming from the short-range part, i.e.,

$$\int_{R_1}^{R_{\rm dip}} p(R)\, dR = \left(v_0 + \frac{1}{2}\right)\pi. \tag{20}$$

Shimamura [31] derived the relation of Eq. (19) using the analytic property of the modified Bessel function, which represents the solution for the dipole potential. In a precise sense, only if $\Omega < -1/4$ can the potential tail $\Omega/(2\mu R^2)$ support an infinite number of bound states [33]. In the $\bar{p} + {\rm H}(1,0,0)$ system, the condition of $\Omega < -1/4$ still gives $J \leqslant 73$.

III. ELECTRON DETACHMENT

In the $\bar{p} + {\rm H}$ system, the electron cannot be bound at small distances $R \leqslant A_{n_1 n_2 \lambda}$, and the electron detachment (autodetachment for the molecular system) is considered a critical decay process. As a practical matter, the electron detachment would be significantly promoted even at distances much larger than $A_{n_1 n_2 \lambda}$. Therefore, it would be useful if one could define the minimum distance R_0 ($> A_{n_1 n_2 \lambda}$) such that the electron detachment occurs rarely at $R > R_0$: If the vibrational region is outside the range R_0, the vibrational state is expected to be sufficiently stable against autodetachment, and to be reasonably described by the BO approximation. Several studies tried to make a rough estimate of R_0 so far by introducing a diabatic representation or by carrying out a $\bar{p} + {\rm H}$ collision calculation, and suggested $R_0 \sim 1.5$ a.u. for the electronic ground state [30,38,39]. In this section, the stability of $\bar{p}{\rm H}$ is discussed by using $V_{\rm eff}(R)$ and R_0.

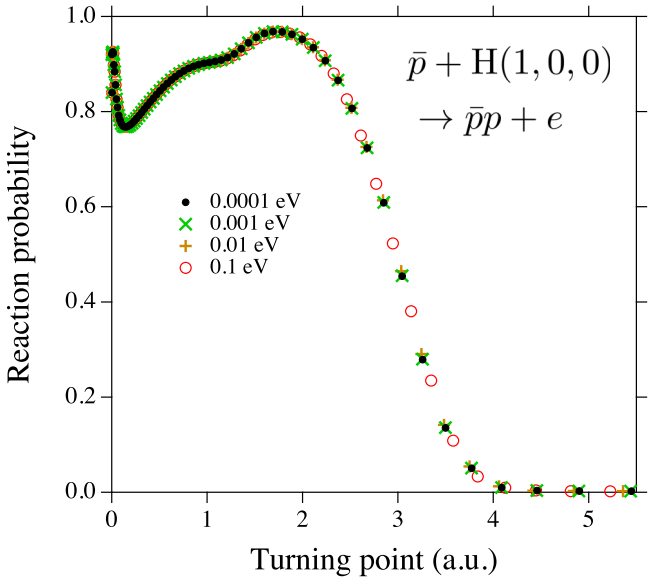

FIG. 4. Reaction probabilities of $\bar{p} + {\rm H}(1,0,0) \to \bar{p}p + e$ plotted as a function of the classical turning point of the $\bar{p} + {\rm H}$ radial motion at collision energies of 0.0001–0.1 eV [32].

Figure 2 shows several effective potentials $V_{\rm eff}(R)$ for the electronic ground state (0,0,0). The cut of the potential curve exists at $R = R_{\rm FT}$. Figure 2 indicates that the vibrational region moves outward with increasing J, although the effective potential with too high J ($\geqslant$30) cannot support vibrational levels below the dissociation limit $-1/2$ a.u. ($n = 1$). It seems that the vibrational states may be supported for $J = 26$–29. However, the value of $R_0 \sim 1.5$ a.u. excludes the possibility of the vibrational motion for all J. Actually in a rigorous calculation, any stable and even metastable vibrational states with high J could not be found [25]. A peculiar case is very high vibration just below the dissociation limit for $J \sim 0$ [25]. In this case, although the electron detachment and pair annihilation occur at small distances, the vibrational wave function can still have finite amplitudes even up to very large distances $R \sim 100$ a.u. This vibrational motion is highly unstable and has a very short lifetime ($<10^{-12}$ s) [25].

Figure 3 shows the effective potentials for the electronic excited state (1,0,0). As is expected, the effective potential can support vibrational levels even for very high J ($\leqslant J_{\rm max} = 73$), and the vibrational motion occurs in the distant region ($R \gg 1$). It should be pointed out, however, that the distance R_0 for electronically excited H would be much longer than that ($\sim$1.5 a.u.) for H($1s$). To estimate the value of R_0 in $\bar{p} + {\rm H}(1,0,0)$, a previous calculation of the reaction $\bar{p} + {\rm H}(n = 2) \to \bar{p}p + e$ [32] is helpful. In this calculation, a semiclassical impact-parameter method was employed. Accordingly, one can plot the probability of the detachment reaction as a function of the classical turning point of the $\bar{p} + {\rm H}$ radial motion. Figure 4 shows such results for H(1, 0, 0) at collision energies of 0.0001–0.1 eV [32], and suggests $R_0 \sim 4$ a.u. Then, choosing $R > 4$ a.u. as the stable region in

Fig. 3 indicates that the effective potentials with high angular momenta $60 \lesssim J \leqslant 73$ are favorable and can support stable vibrational states. Actually, the electron detachment cannot necessarily be neglected even for high J, and the vibrational states with $60 \lesssim J \leqslant 73$ would have finite (but sufficiently long) lifetimes due to autodetachment. Such autodetachment decays are fully investigated in Sec. IV D.

For the other electronic excited states $(0, 0, \pm 1)$ and (0,1,0) shown in Fig. 1, the BO potential has no long-range attractive $(\propto -1/R^2)$ term, and additionally the critical distances $A_{n_1 n_2 \lambda}$ are much longer: Thereby, the related effective potentials are always above the dissociation limit $-1/8$ a.u. at $R > A_{n_1 n_2 \lambda}$. The $(0, 0, \pm 1)$ and (0,1,0) states cannot support any stable vibrational motion, and they are of no concern in the present study.

In Ref. [25], which is a full quantum-mechanical treatment based on an R-matrix method, the electron detachment process for $\bar{p}\mathrm{H}(0, 0, 0)$ was calculated rigorously without assuming the BO approximation. One may expect that the R-matrix method is also applicable to $\bar{p}\mathrm{H}(1, 0, 0)$. However, it is not easy to carry out the R-matrix calculation for $\bar{p}\mathrm{H}(1, 0, 0)$, because the R-matrix diagonalization relevant to a more extended spacial domain is required for the large value of R_0, and a huge number of very high R-matrix diagonalized states are required for the electronic excited molecule. The semiclassical approximation [32] is free from such limitations, but it is not suitable for an accurate description of the molecular vibration. In the present study, since only the region of $R \gg A_{n_1 n_2 \lambda}$ is related to the vibrational state, an approach based on the BO approximation is appropriate.

IV. $\bar{p}$H MOLECULES IN THE (1, 0, 0) STATE

In this section, the discussion is given specifically for the first electronic excited state $(n_1, n_2, \lambda) = (1, 0, 0)$ of the $\bar{p}$H molecule, which has asymptotically the attractive long-range term $\propto -1/R^2$ in the BO potential. As shown in Sec. III, the existence of the vibrational states of the $\bar{p}\mathrm{H}(1, 0, 0)$ molecule is promising. First, the vibrational energy levels of $\bar{p}\mathrm{H}(1, 0, 0)$ are calculated on the basis of the BO approximation and by neglecting the decay processes. The most important decay channel is the autodetachment. For other atomic decay channels, the predissociation and the spontaneous radiative dissociation are considered. Here, perturbation treatments are presented for calculating the energy widths of the vibrational levels attributable to the decay processes. Since high angular momenta are considered for the $\bar{p}$H rotation, the annihilation decay can be neglected.

A. Vibrational bound states

By neglecting all the decay channels, the bound-state wave function of the $\bar{p}$H molecule in the $(n_1, n_2, \lambda) = (1, 0, 0)$ state may be expressed by

$$\Phi^{100}_{vJM}(\mathbf{R}, \mathbf{r}) = R^{-1} \mathcal{D}^J_{M0}(\hat{\mathbf{R}}) F_{vJ}(R) \chi_{100}(R; \mathbf{r}), \tag{21}$$

where

$$\mathcal{D}^J_{M\lambda}(\hat{\mathbf{R}}) = \left(\frac{2J+1}{4\pi}\right)^{1/2} \left[D^J_{M\lambda}(\hat{\mathbf{R}})\right]^* \tag{22}$$

is the normalized form of the Wigner D-function $D^J_{M\lambda}$, and $R^{-1}F_{vJ}(R)$ is normalized to unity: $\langle R^{-1}F_{v'J}|R^{-1}F_{vJ}\rangle_R = \delta_{v'v}$, with v being the vibrational quantum number. Rather than Eq. (11), here the equation of vibrational motion is given by considering

$$\left\langle \mathcal{D}^J_{M0}\chi_{100}\middle| H - E \middle|\Phi^{100}_{vJM}\right\rangle_{\hat{\mathbf{R}}\mathbf{r}} = 0, \tag{23}$$

with the total energy

$$E = E_{vJ} - \frac{1}{8}, \tag{24}$$

where E_{vJ} is the vibrational energy ($E_{vJ} \to 0$ as $v \to \infty$). Equation (23) becomes

$$\left[-\frac{1}{2\mu}\frac{d^2}{dR^2} + \frac{J(J+1) + \langle\chi_{100}|\mathbf{l}^2|\chi_{100}\rangle_{\mathbf{r}}}{2\mu R^2} - \frac{1}{2\mu}\langle\chi_{100}|\frac{d^2}{dR^2}|\chi_{100}\rangle_{\mathbf{r}} + V_{100}(R) + \frac{1}{8}\right] F_{vJ}(R) = E_{vj} F_{vJ}(R), \tag{25}$$

which includes the diagonal parts of nonadiabatic coupling matrix elements $\langle\chi_{n_1' n_2' \lambda'}|\mathbf{l}^2|\chi_{n_1 n_2 \lambda}\rangle_{\mathbf{r}}$ and $\langle\chi_{n_1' n_2' \lambda'}|d^2/dR^2|\chi_{n_1 n_2 \lambda}\rangle_{\mathbf{r}}$ other than the expression of Eq. (11). The nondiagonal matrix elements closely relevant to the (1,0,0) state are those of the coupling with the next higher states $(0, 0, \pm 1)$ and (0,1,0) and with the ground state (0,0,0). As mentioned previously, the high-J effective potential curves for the $(0, 0, \pm 1)$ and (0,1,0) states are above the dissociation limit of $\bar{p} + \mathrm{H}(n = 2)$. Thus, the couplings with the $(0, 0, \pm 1)$, (0,1,0), and still higher electronic states are less significant, and they are neglected in the present study. Because of the nonadiabatic coupling with the (0,0,0) state, the $\bar{p}\mathrm{H}(1, 0, 0)$ molecule cannot be permanently stable, and it has a decay channel of predissociation, which is discussed in Sec. IV B.

To obtain the nonadiabatic coupling matrix elements, Eq. (7) was solved by using a discrete-variable-representation (DVR) method in polar coordinates [40,41]: 90-point Laguerre meshes for the radial coordinate r, and 6-point Legendre meshes for the polar angle of $\mathbf{r}$. To check the accuracy of this calculation, the adiabatic electron energies obtained in the present study are compared with the accurate ones of Wallis *et al.* [29] in Table I. In calculating the coupling matrix

TABLE I. Adiabatic electron energies $\Lambda_{n_1 n_2 \lambda}(R)$ of $\bar{p} + \mathrm{H}$ for $(n_1, n_2, \lambda) = (1, 0, 0)$: the accurate results of Wallis *et al.* [29] and the present DVR results.

R (a.u.)	Wallis *et al.* (a.u.)	Present (a.u.)
3.0	-4.2187×10^{-3}	-4.2072×10^{-3}
5.0	-1.8990×10^{-2}	-1.8953×10^{-2}
10.0	-5.1862×10^{-2}	-5.1804×10^{-2}
15.0	-7.0682×10^{-2}	-7.0622×10^{-2}
20.0	-8.2053×10^{-2}	-8.1992×10^{-2}
25.0	-8.9555×10^{-2}	-8.9495×10^{-2}
30.0	-9.4851×10^{-2}	-9.4791×10^{-2}

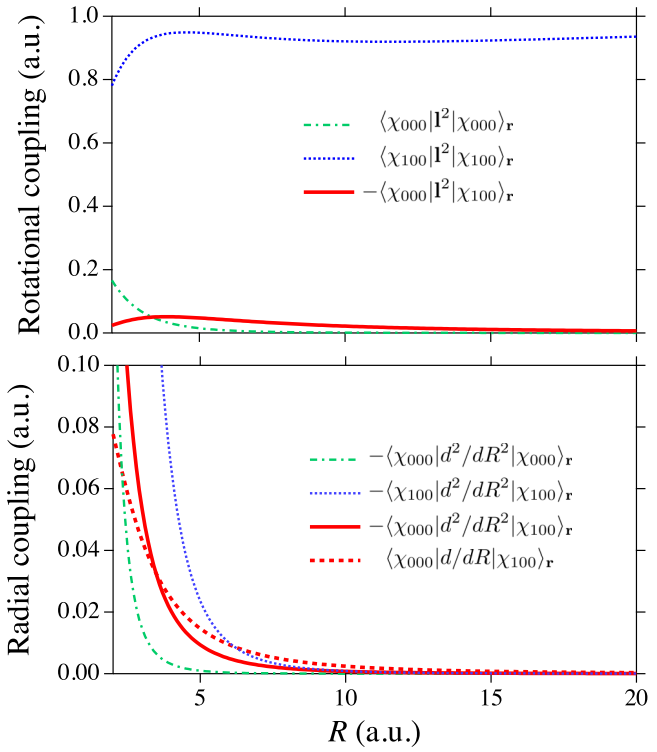

FIG. 5. Nonadiabatic (rotational and radial) coupling matrix elements, related to $(n_1, n_2, \lambda) = (0, 0, 0)$ and (1,0,0), plotted as a function of R.

elements, the following relations were used:

$$\langle\chi_{\gamma'}|\frac{d}{dR}|\chi_{\gamma}\rangle_{\mathbf{r}} = -\frac{1}{V_{\gamma'}(R) - V_{\gamma}(R)}\langle\chi_{\gamma'}|\frac{\partial H_{\rm BO}}{\partial R}|\chi_{\gamma}\rangle_{\mathbf{r}},$$

$$\langle\chi_{\gamma'}|\frac{d^2}{dR^2}|\chi_{\gamma}\rangle_{\mathbf{r}} = \sum_{\gamma''}\langle\chi_{\gamma'}|\frac{d}{dR}|\chi_{\gamma''}\rangle_{\mathbf{r}}\langle\chi_{\gamma''}|\frac{d}{dR}|\chi_{\gamma}\rangle_{\mathbf{r}} + \frac{d}{dR}\langle\chi_{\gamma'}|\frac{d}{dR}|\chi_{\gamma}\rangle_{\mathbf{r}},$$

where γ abbreviates (n_1, n_2, λ). Figure 5 shows the nonadiabatic coupling matrix elements related to $(n_1, n_2, \lambda) = (0, 0, 0)$ and (1,0,0). One can see that the nonadiabatic coupling is weak unless R is small. In the present calculation, the BO potential data of Wallis *et al.* [29] were used, and the cubic spline interpolation was applied to the values at distances not reported by them. Table II shows the lowest ($v = 0$) vibrational energies for $J = 50$–70, calculated by using Eq. (11) of the BO approximation and by using Eq. (25) of the BO approximation with the nonadiabatic correction, which is found to yield only a minor (0.2–0.6 %) contribution.

B. Predissociation

The nonadiabatic coupling induces the dynamical transition $(n_1, n_2, \lambda) = (1, 0, 0) \rightarrow (0, 0, 0)$. As seen in Fig. 6, the high-J vibrational levels of $\bar{p}$H$(1, 0, 0)$ are always far above the dissociation limit of $\bar{p} + \mathrm{H}(1s)$. Therefore, due to the nonadiabatic coupling, the $\bar{p}$H$(1, 0, 0)$ molecule decays into

TABLE II. The lowest ($v = 0$) vibrational energies of the $\bar{p}$H molecule in the first electronic excited state (1,0,0) for $J = 50$–70, obtained from Eqs. (11) and (25). $L_{\rm max}$ is the largest angular momentum quantum number of the $\bar{p}p$ atom such that the $\bar{p}p$ energy is lower than $E_{v=0,J} - 1/8$. The parameter $l_0 = J - L_{\rm max}$, necessary for the discussion about autodetachment, is also shown.

J	$E_{\rm BO}$ (eV)	$E_{v=0,J}$ (eV)	$L_{\rm max}$	l_0
50	−1.5109	−1.5052	49	1
51	−1.3476	−1.3429	50	1
52	−1.1967	−1.1928	51	1
53	−1.0575	−1.0542	51	2
54	−0.92939	−0.92669	52	2
55	−0.81176	−0.80951	53	2
56	−0.70407	−0.70220	54	2
57	−0.60582	−0.60427	54	3
58	−0.51652	−0.51524	55	3
59	−0.43576	−0.43469	56	3
60	−0.36310	−0.36223	56	4
61	−0.29818	−0.29746	57	4
62	−0.24062	−0.24003	57	5
63	−0.19008	−0.18961	57	6
64	−0.14625	−0.14587	58	6
65	−0.10881	−0.10851	58	7
66	−0.077472	−0.077240	58	8
67	−0.051959	−0.051785	59	8
68	−0.032002	−0.031877	59	9
69	−0.017331	−0.017246	59	10
70	−0.0076283	−0.0075788	59	11

dissociative continua in the electronic ground state:

$$\bar{p}\mathrm{H}(v, J) \rightarrow \bar{p} + \mathrm{H}(1s). \tag{26}$$

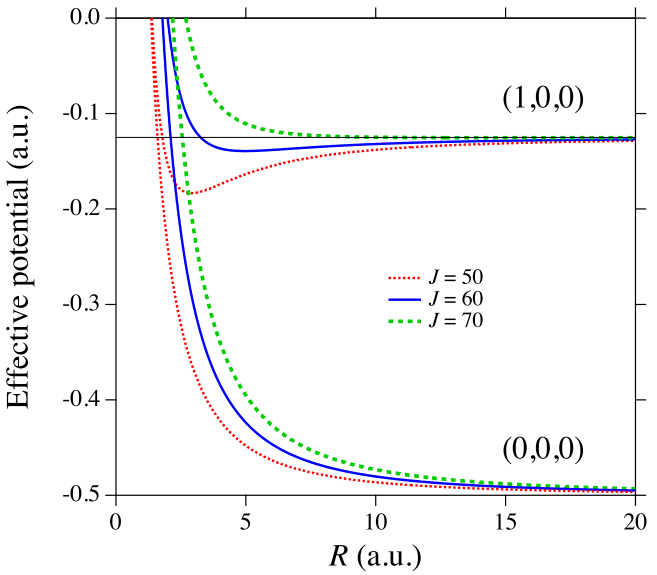

FIG. 6. Effective potentials $V_{\rm eff}(R) = J(J+1)/(2\mu R^2) + V_{n_1 n_2 \lambda}(R)$ relevant to the predissociation $(n_1, n_2, \lambda) = (1, 0, 0) \rightarrow (0, 0, 0)$ of $\bar{p}$H. The total angular momentum is $J = 50$, 60, and 70.

This process is known as predissociation, and the conservation of the total energy E is

$$E = E_{vJ} - \frac{1}{8} = \mathcal{E} - \frac{1}{2}, \tag{27}$$

where $\mathcal{E}$ is the kinetic energy of $\bar{p} + \mathrm{H}(1s)$.

The present system shows no notable avoided-crossing (Fig. 6), and the nonadiabatic coupling is very weak except at small distances (Fig. 5). Therefore, the predissociation is expected to be very slow. The energy width attributable to predissociation [42] is given by

$$\Gamma_{\mathrm{dis}} = \frac{4\mu}{k}|T_{\mathrm{dis}}|^2, \tag{28}$$

with $k = \sqrt{2\mu\mathcal{E}}$ and

$$T_{\mathrm{dis}} = \left\langle \Phi^{000}_{\mathcal{E}JM} \middle| H \middle| \Phi^{100}_{vJM} \right\rangle, \tag{29}$$

where $\langle\ |\ |\ \rangle$ indicates the integration over all the coordinates $(\mathbf{R}, \mathbf{r})$. The wave function of the final dissociative-continuum state is expressed by

$$\Phi^{000}_{\mathcal{E}JM}(\mathbf{R}, \mathbf{r}) = R^{-1}\mathcal{D}^{J}_{M0}(\hat{\mathbf{R}})G_{\mathcal{E}J}(R)\chi_{000}(R; \mathbf{r}), \tag{30}$$

where the radial function $G_{\mathcal{E}J}(R)$ is given by solving

$$\begin{aligned}\Bigg[-\frac{1}{2\mu}\frac{d^2}{dR^2} + \frac{J(J+1) + \langle\chi_{000}|\mathbf{l}^2|\chi_{000}\rangle_{\mathbf{r}}}{2\mu R^2} \\ - \frac{1}{2\mu}\langle\chi_{000}|\frac{d^2}{dR^2}|\chi_{000}\rangle_{\mathbf{r}} + V_{000}(R) + \frac{1}{2}\Bigg]G_{\mathcal{E}J}(R) \\ = \mathcal{E}G_{\mathcal{E}J}(R),\end{aligned} \tag{31}$$

and it is assumed to have the asymptotic form

$$G_{\mathcal{E}J}(R) \xrightarrow[R\to\infty]{} \sin(kR + \eta), \tag{32}$$

with η being a constant phase. Explicitly, Eq. (29) becomes

$$\begin{aligned}T_{\mathrm{dis}} = &-\frac{1}{2\mu}\int_0^\infty G_{\mathcal{E}J}(R)\langle\chi_{000}|\frac{d^2}{dR^2}|\chi_{100}\rangle_{\mathbf{r}}\, F_{vJ}(R)\, dR \\ &+ \frac{1}{2\mu}\int_0^\infty G_{\mathcal{E}J}(R)\frac{1}{R^2}\langle\chi_{000}|\mathbf{l}^2|\chi_{100}\rangle_{\mathbf{r}}\, F_{vJ}(R)\, dR \\ &- \frac{1}{\mu}\int_0^\infty G_{\mathcal{E}J}(R)\langle\chi_{000}|\frac{d}{dR}|\chi_{100}\rangle_{\mathbf{r}}\frac{dF_{vJ}}{dR}(R)\, dR.\end{aligned} \tag{33}$$

C. Spontaneous radiative dissociation

The radiative transition between the electronic states $(n_1, n_2, \lambda) = (1, 0, 0)$ and (0,0,0) is optically allowed. As can be seen in Fig. 6, since no potential well exists in the (0,0,0) effective potential for high J, the spontaneous radiative emission of the $\bar{p}\mathrm{H}(1, 0, 0)$ molecule always leads to the dissociation:

$$\bar{p}\mathrm{H}(v, J) \to \bar{p} + \mathrm{H}(1s) + h\nu, \tag{34}$$

which brings about a continuum photon emission. In this case, the energy conservation becomes

$$E = E_{vJ} - \frac{1}{8} = \mathcal{E} - \frac{1}{2} + h\nu, \tag{35}$$

where $h\nu$ is the photon energy, and the $\bar{p} + \mathrm{H}(1s)$ kinetic energy $\mathcal{E}$ varies over a range of 0 to $E + 1/2$.

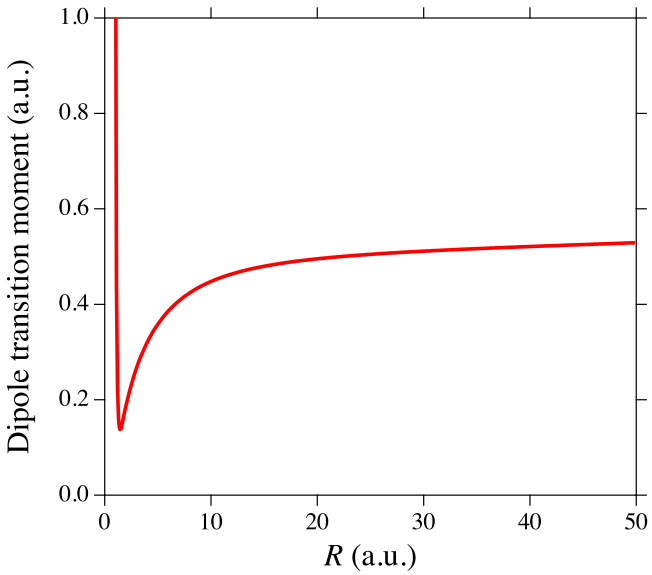

FIG. 7. Electronic dipole moment $D(R)$ for the (1, 0, 0)-(0, 0, 0) transition of $\bar{p}\mathrm{H}$ as a function of R. In the separated atom limit, $D(\infty) = 0.527$ a.u.

For the energy width attributable to spontaneous radiative dissociation, perturbation theory [43] gives

$$\Gamma_{\mathrm{rad}} = \int_0^{E+1/2} \omega(\mathcal{E})\, d\mathcal{E}, \tag{36}$$

where

$$\omega(\mathcal{E}) = \frac{8\mu}{3\pi k c^3}\left(E - \mathcal{E} + \frac{1}{2}\right)^3 \frac{1}{2J+1}\sum_{J'M'M}|T_{\mathrm{rad}}|^2, \tag{37}$$

with c being the speed of light, and

$$T_{\mathrm{rad}} = \left\langle \Phi^{000}_{\mathcal{E}J'M'} \middle| z \middle| \Phi^{100}_{vJM} \right\rangle. \tag{38}$$

Equation (37) has the P- and R-branch contributions: i.e.,

$$\begin{aligned}\sum_{J'M'M}|T_{\mathrm{rad}}|^2 = \Bigg[(J+1)\left|\int_0^\infty G_{\mathcal{E},J+1}(R)D(R)F_{vJ}(R)dR\right|^2 \\ + J\left|\int_0^\infty G_{\mathcal{E},J-1}(R)D(R)F_{vJ}(R)dR\right|^2\Bigg],\end{aligned} \tag{39}$$

where

$$D(R) = \langle\chi_{000}|z|\chi_{100}\rangle_{\mathbf{r}} \tag{40}$$

is the electronic dipole transition moment.

Figure 7 shows the electronic dipole moment $D(R)$ for the (0, 0, 0)-(1, 0, 0) transition. In the separated atom limit, the dipole moment becomes $D(\infty) = \langle 1s|z|2p_0\rangle/\sqrt{2} = 0.527$ a.u. Except at small distances, the dipole moment $D(R)$ increases monotonically with R, and it is lower than $D(\infty)$.

D. Autodetachment

As mentioned in Sec. III, the $\bar{p}\mathrm{H}$ molecule in the $(n_1, n_2, \lambda) = (1, 0, 0)$ state has a finite lifetime due to autodetachment:

$$\bar{p}\mathrm{H}(v, J) \to \bar{p}p(N, L) + e, \tag{41}$$

where (N, L) is the principal and angular momentum quantum numbers of the $\bar{p}p$ atom, and $0 \leqslant L \leqslant N-1$. The total energy is represented as

$$E = E_{vJ} - \frac{1}{8} = E_N + \epsilon, \tag{42}$$

where $E_N = -\mu/(2N^2)$ is the energy of $\bar{p}p(N, L)$, and ϵ is the kinetic energy of the detached electron. In the present study, because of $E < 0$, the breakup channel ($\rightarrow \bar{p} + p + e$) is closed. The autodetachment decay can also be considered as the nonadiabatic process. However, since the final electronic states are continua, it is not clever to calculate the autodetachment decay width by using the nonadiabatic treatment as in Sec. IV B. Fortunately, the essential part of the dynamical mechanism of the autodetachment is quite similar to that of the Auger transition of antiprotonic atoms [9,31,44–46]. It is found furthermore that conventional perturbation treatment is sufficiently accurate for this Auger decay process [9,45]. Since the autodetachment decay rate is expected to be low for high J, the present study employs the conventional perturbation theory.

The energy width attributable to autodetachment is given by

$$\Gamma_{\rm det} = \sum_{NLl} \Gamma_{\rm det}(N, L, l), \tag{43}$$

where l is the orbital angular momentum of the detached electron, and the partial width is

$$\Gamma_{\rm det}(N, L, l) = \frac{4}{\kappa}|T_{\rm det}(N, L, l)|^2, \tag{44}$$

with $\kappa = \sqrt{2\epsilon}$. Perturbation theory [45] gives

$$T_{\rm det}(N, L, l) = \left\langle \Psi^{JM}_{NLl} \middle| H - E \middle| \Phi^{100}_{vJM} \right\rangle. \tag{45}$$

The wave function Ψ^{J}_{NLl} for the final state is given by

$$\Psi^{JM}_{NLl}(\mathbf{R}', \mathbf{r}') = R^{-1}\mathcal{Y}^{JM}_{Ll}(\hat{\mathbf{R}}', \hat{\mathbf{r}}')\Upsilon_{NL}(R) f_{\epsilon l}(r), \tag{46}$$

where $(\mathbf{R}', \mathbf{r}')$ are described in the space-fixed frame,

$$\mathcal{Y}^{JM}_{Ll}(\hat{\mathbf{R}}', \hat{\mathbf{r}}') = \sum_{m_L m_l} (Lm_L l m_l | JM) Y_{Lm_L}(\hat{\mathbf{R}}') Y_{lm_l}(\hat{\mathbf{r}}') \tag{47}$$

is the eigenfunction of the total angular momentum (J, M), $R^{-1}\Upsilon_{NL}(R)$ is the radial (Coulomb) wave function of $\bar{p}p(N, L)$, and $f_{\epsilon l}(r) = \kappa j_l(\kappa r)$, with j_l being the spherical Bessel function, represents the continuum state of the detached electron. In Eq. (47), $(\ |\ )$ is the Clebsch-Gordan coefficient, and Y_{Lm} is the spherical harmonics.

To calculate Eq. (45), first one should notice the following relation between the space-fixed and body-fixed angular basis functions [47]:

$$\mathcal{Y}^{JM_J}_{Ll}(\hat{\mathbf{R}}', \hat{\mathbf{r}}') = \sum_{\lambda} U^{Jl}_{L\lambda} \mathcal{D}^{J}_{M_J\lambda}(\hat{\mathbf{R}}) Y_{l\lambda}(\hat{\mathbf{r}}), \tag{48}$$

with

$$U^{Jl}_{L\lambda} = \left(\frac{2L+1}{2J+1}\right)^{1/2} (L0l\lambda|J\lambda). \tag{49}$$

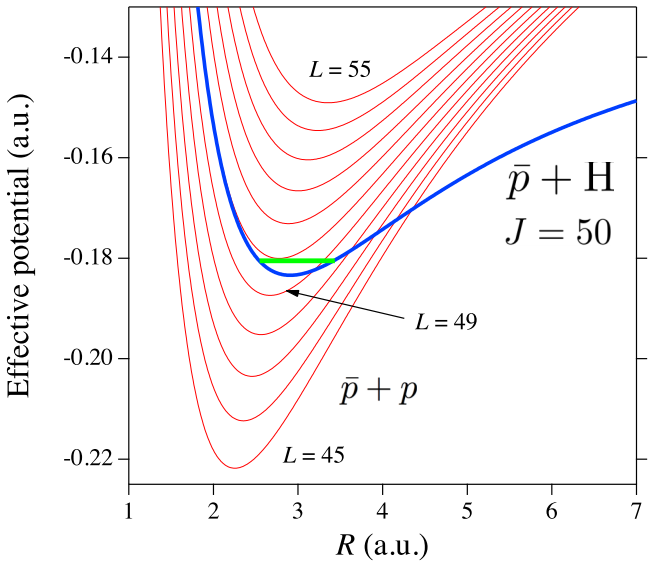

FIG. 8. Effective potentials relevant to the autodetachment $\bar{p}\mathrm{H}(v, J) \rightarrow \bar{p}p(N, L) + e$: $V_{\rm eff}(R) = J(J+1)/(2\mu R^2) + V_{100}(R)$ of $\bar{p}\mathrm{H}$ for $J = 50$, and $L(L+1)/(2\mu R^2) - 1/R$ of $\bar{p}p$ for $L =$ 45–55. The horizontal line indicates the lowest ($v = 0$) vibrational energy level of $\bar{p}\mathrm{H}$ ($J = 50$), and the vibrational region is $2.5 \lesssim R \lesssim$ 3.4 a.u., which is inside the range R_0.

Then, one can easily perform the integration over $\hat{\mathbf{R}}$ in Eq. (45): i.e.,

$$T_{\rm det}(N, L, l) = U^{Jl}_{L0} \int_0^\infty \Upsilon_{NL}(R) t_{\epsilon l}(R) F_{vJ}(R) dR, \tag{50}$$

where

$$t_{\epsilon l}(R) = \langle Y_{l0} f_{\epsilon l}| - \frac{1}{r} + \frac{1}{|\mathbf{R} - \mathbf{r}|} |\chi_{100}\rangle_{\mathbf{r}}. \tag{51}$$

Due to the factor U^{Jl}_{L0}, the detachment can take place only for $J + L + l =$ even. The BO wave function $\chi_{100}(R; \mathbf{r})$ was calculated by using the present DVR method, as described in Sec. IV A.

Figure 8 shows the effective potential of $\bar{p}\mathrm{H}(1, 0, 0)$ with $J = 50$ and its lowest ($v = 0$) vibrational energy level. This is the case in which the vibrational region is inside $R = R_0$. In Eq. (42), because of $\epsilon > 0$, the $\bar{p}p$ energy must be $E_N < E_{vJ} - 1/8$. Therefore, in the autodetachment of $\bar{p}\mathrm{H}(v = 0, J = 50)$, the final product $\bar{p}p(N, L)$ must have $L \leqslant 49$. The critical importance is whether the final states of $L \simeq J$ are energetically allowed [9,31,44,46]: Since the detached electron can carry away only low angular momenta l, the restriction $l \geqslant |J - L|$ implies that the autodetachment would be very slow unless the difference $|J - L|$ is small. Table II shows $L_{\rm max}$, which is the highest angular momentum L such that $E_{v=0,J} - 1/8 > E_N$. Since the relation $l \geqslant J - L \geqslant J - L_{\rm max} > 0$ is always satisfied for the open channels associated with $v = 0$, the difference $l_0 = J - L_{\rm max}$ (also shown in Table II) is a basic parameter for measuring the importance of the autodetachment. For $J = 50$ (Fig. 8), the small value of $l_0 = 1$ means that the autodetachment can be highly promoted. It is seen in Fig. 8 furthermore that the Franck-Condon overlap integral is also huge between

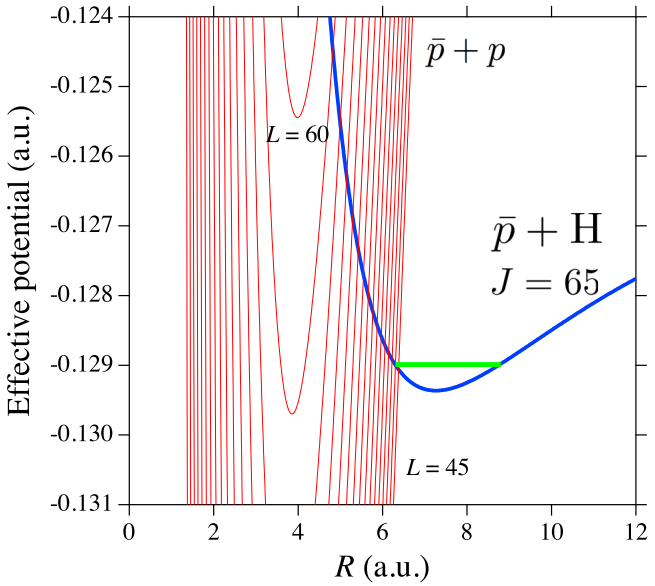

FIG. 9. Effective potentials relevant to the autodetachment $\bar{p}\mathrm{H}(v,J)\to\bar{p}p(N,L)+e$: $V_{\mathrm{eff}}(R)=J(J+1)/(2\mu R^2)+V_{100}(R)$ of $\bar{p}\mathrm{H}$ for $J=65$, and $L(L+1)/(2\mu R^2)-1/R$ of $\bar{p}p$ for $L=45$–60. The horizontal line indicates the lowest ($v=0$) vibrational energy level of $\bar{p}\mathrm{H}(J=65)$, and the vibrational region is $6.3\lesssim R\lesssim 8.8$ a.u., which is outside the range R_0.

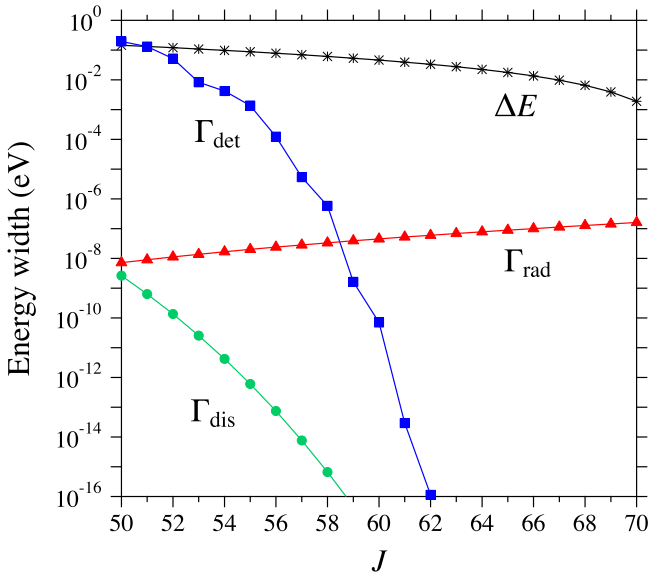

FIG. 10. Energy widths of $\bar{p}\mathrm{H}(v=0,J)$ for $J=50$–70, attributable to predissociation (Γ_{dis}), spontaneous radiative dissociation (Γ_{rad}), and autodetachment (Γ_{det}). Vibrational energy differences $\Delta E=E_{v=1,J}-E_{v=0,J}$ are also plotted.

$\bar{p}\mathrm{H}(v=0,J=50)$ and $\bar{p}p(N,L=49)$. This fact firmly establishes the high rate of autodetachment for $\bar{p}\mathrm{H}(v=0,J=50)$.

Figure 9 shows the effective potential for $\bar{p}\mathrm{H}(J=65)$ and the lowest ($v=0$) vibrational energy level. In this case, the vibrational region is outside $R=R_0$. In contrast to $\bar{p}\mathrm{H}(J=50)$, the energetically allowed states of $\bar{p}p$ are $L\leqslant L_{\max}=58$; namely, the value of $l_0=7$ is very large. Furthermore, the Franck-Condon factor between $\bar{p}\mathrm{H}(v=0,J=65)$ and $\bar{p}p(N,L\gg 45)$ is negligibly small. The autodetachment would be very slow for $\bar{p}\mathrm{H}(v=0,J=65)$. Generally, one can expect that the autodetachment rate becomes lower with increasing J. Incidentally, the effective potentials relevant to the autodetachment of $\bar{p}\mathrm{H}(0,0,0)$ with $J\leqslant 31$ (cf., Fig. 2) have features that are essentially the same as those seen in Fig. 8 and not in Fig. 9. This demonstrates that the autodetachment rate of $\bar{p}\mathrm{H}(0,0,0)$ is always very high.

V. DECAY WIDTHS AND LIFETIMES

Figure 10 shows the predissociation widths Γ_{dis} calculated by Eq. (28) for $\bar{p}\mathrm{H}(v=0)$ with $J=50$–70. The width Γ_{dis} is $<10^{-8}$ eV, and it decreases rapidly with increasing J. The predissociation process can be properly described by a straightforward approach based on two-state close coupling (CC): The $\bar{p}\mathrm{H}(1,0,0)$ species are represented as closed-channel resonances in the elastic $\bar{p}+\mathrm{H}(0,0,0)$ collisions. In the present study, the CC calculation was tentatively carried out for $(v,J)=(0,50)$. It offers the same value of the resonance energy as E_{vJ} in the number of digits shown in Table II, and the resonance width is 2.80×10^{-9} eV while Eq. (28) gives $\Gamma_{\mathrm{dis}}=2.65\times 10^{-9}$ eV. This result guarantees the accuracy of the perturbation treatment of Eq. (28). For higher J, unfortunately the CC method becomes inefficient in the numerical calculation because of too narrow resonance widths, and the perturbation treatment would be rather much more suitable. At any rate, the predissociation is found to be always insignificant for $\bar{p}\mathrm{H}(v=0,J\gtrsim 50)$.

Figure 10 also shows the radiation widths Γ_{rad} calculated by Eq. (36) for $\bar{p}\mathrm{H}(v=0)$. The radiation width is $\Gamma_{\mathrm{rad}}\simeq 10^{-8}$–$10^{-7}$ eV for $J=50$–70, and it increases slowly with J. These values are smaller than, but not so different from, the radiation width ($=4.11\times 10^{-7}$ eV) of the isolated $\mathrm{H}(2p)$ atom. Figure 11 shows the energy distribution ω of the emitted photon, which is given by Eq. (37) using the relation $h\nu=E_{vJ}+3/8-\mathcal{E}$. With increasing J, the distribution becomes narrower, and the peak position moves toward the Ly-α line of $\mathrm{H}(2p\to 1s)$. This can be understood by looking at the feature of the effective potential shown in Fig. 6. For higher J, the Franck-Condon region where the vibrational wave function of $\bar{p}\mathrm{H}(1,0,0)$ has a finite amplitude moves to a distant place of larger R, and there the related effective potential of the (0,0,0) state becomes flatter and closer to $-1/2$ a.u.: The steeper R dependence of the (0,0,0) effective potential in the Franck-Condon region makes the energy distribution broader.

Figure 10 further plots the autodetachment widths Γ_{det} calculated by Eq. (43) for $\bar{p}\mathrm{H}(v=0)$. The width Γ_{det} is significantly large for low J, and it decreases tremendously with increasing J: accordingly, $\Gamma_{\mathrm{det}}\gg\Gamma_{\mathrm{rad}}$ for $J\leqslant 58$, and $\Gamma_{\mathrm{rad}}\gg\Gamma_{\mathrm{det}}$ for $J>58$. Figure 10 shows the vibrational energy difference $\Delta E=E_{v=1,J}-E_{v=0,J}$. For $J\sim 50$, since the width Γ_{det} is comparable to ΔE, the perturbation treatment of Eq. (45) is of no use. Although a more sophisticated method should be applied to the autodetachment for such low J, it is evident that the $\bar{p}\mathrm{H}$ molecules with $J\lesssim 50$ only have highly unstable states. In the present calculation, the 6-point Legendre meshes were applied to the polar angle of $\mathbf{r}$. It means that the electronic angular momenta of $l=0,1,\ldots,5$

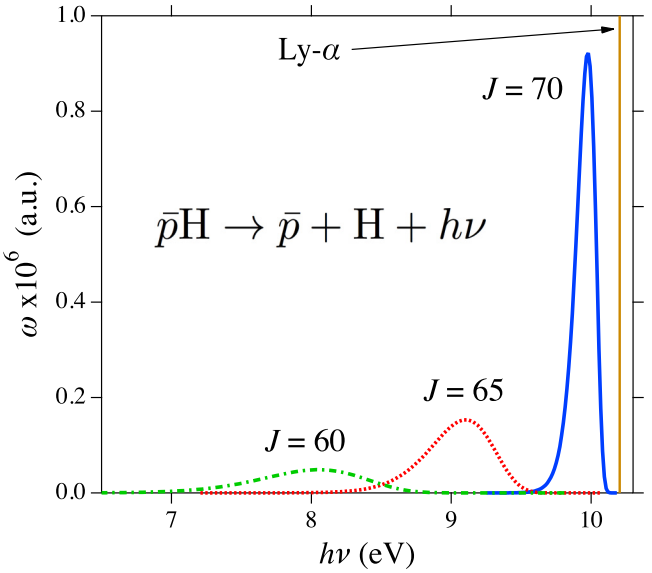

FIG. 11. Distributions ω of the emitted photon energy $h\nu$ ($h\nu = E_{vJ} + 3/8 - \mathcal{E}$) in the spontaneous radiative dissociation of $\bar{p}\mathrm{H}(v = 0, J)$ for $J = 60$, 65, and 70. The position of the Ly-α line is indicated.

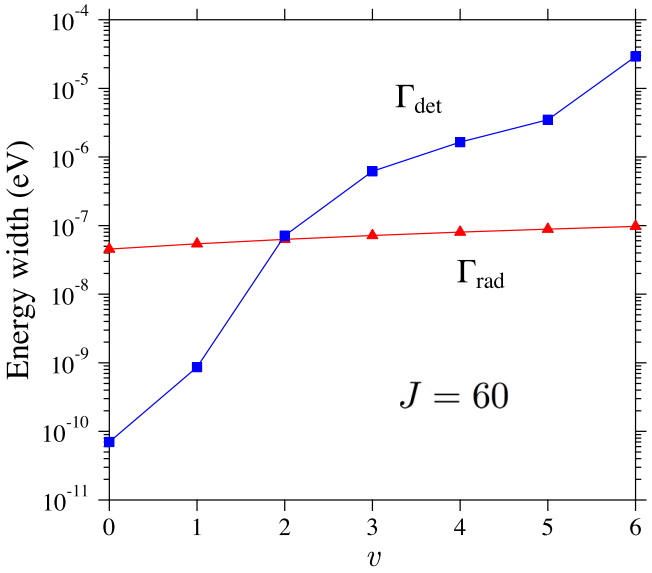

FIG. 13. Energy widths of $\bar{p}\mathrm{H}(v, J=60)$ for $v = 0$–6, attributable to spontaneous radiative dissociation (Γ_{rad}) and autodetachment (Γ_{det}).

are taken into account, and that no transition occurs for $l_0 = J - L_{\max} \geqslant 6$. From Table II, one can see that the autodetachment makes no contribution to the decay of $\bar{p}\mathrm{H}(v=0, J \geqslant 63)$ in the present calculation.

The J dependence of Γ_{det} shown in Fig. 10 is slightly crank: there seems to be a small dip at $J = 53, 57$, and 59. The L-state distribution of $\bar{p}p$ in the autodetachment is reflected in this structure. Figure 12 shows the L-state distribution,

$$\Omega(L) = \frac{1}{\Gamma_{\mathrm{det}}} \sum_{Nl} \Gamma_{\mathrm{det}}(N, L, l). \tag{52}$$

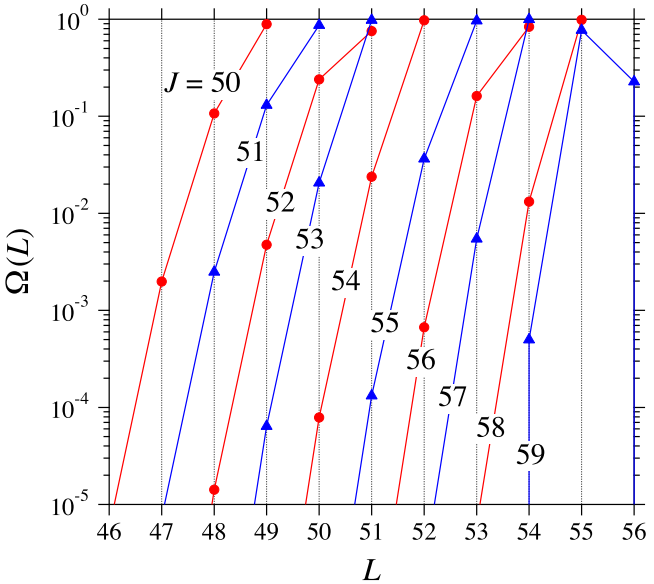

FIG. 12. L-state distributions $\Omega(L) = \Gamma_{\mathrm{det}}(L)/\Gamma_{\mathrm{det}}$, with $\Gamma_{\mathrm{det}}(L) = \sum_{Nl} \Gamma_{\mathrm{det}}(N, L, l)$, in the autodetachment of $\bar{p}\mathrm{H}(v=0, J)$ for $J = 50$–59.

For example, the highest allowed L is the same ($L_{\max} = 51$) in both autodetachment processes with $J = 52$ and 53 (see also Table II). As a result, the important final channel of $l = 1$ is missing for $J = 53$ and not for $J = 52$. This makes the width Γ_{det} for $\bar{p}\mathrm{H}(v=0, J=53)$ relatively smaller than expected. The same thing happens also for $J = 56$ and 57. In the autodetachment processes with $J = 58$ and 59, the values of $L_{\max}$ are different ($L_{\max} = 55$ and 56, respectively). However, the Franck-Condon factor is very small between $\bar{p}\mathrm{H}(v = 0, J = 59)$ and $\bar{p}p(N, L = 56)$, and this makes the fraction $\Omega(L = 56)$ less significant in the autodetachment with $J = 59$ (Fig. 12). This is the origin of the dip in Γ_{det} at $J = 59$.

The v dependence of the energy widths Γ_{rad} and Γ_{det} is shown in Fig. 13 for $\bar{p}\mathrm{H}(J = 60)$. The v dependence is much stronger for Γ_{det} than for Γ_{rad}: accordingly, $\Gamma_{\mathrm{rad}} \gg \Gamma_{\mathrm{det}}$ for $v < 2$, and $\Gamma_{\mathrm{det}} \gg \Gamma_{\mathrm{rad}}$ for $v > 2$. Figure 14 shows the effective potential of $\bar{p}\mathrm{H}(J = 60)$ and several ($v = 0$–5) vibrational energy levels. In the autodetachment, as v increases, the final channels with smaller $|J - L|$ become open, and furthermore the Franck-Condon factor between the related states becomes more significant. This is the reason for the strong v-dependence of Γ_{det} for $J = 60$.

As for higher J, the effective potential $V_{\mathrm{eff}}(R)$ with $J = 65$ is shown in Fig. 9. At the dissociation limit $E = -1/8$ a.u. (namely, $v \to \infty$), the inner classical turning point is $R_1 = 4.9$ a.u. Hence, the Franck-Condon factor between any vibrational state of $\bar{p}\mathrm{H}(J = 65)$ and any $\bar{p}p$ state with $L \geqslant 60$ is quite small. As J increases further from 65, the Franck-Condon factors between $\bar{p}\mathrm{H}(v, J)$ and $\bar{p}p(N, L)$ with $|J - L| \leqslant 5$ become much smaller and negligible. Thus, one

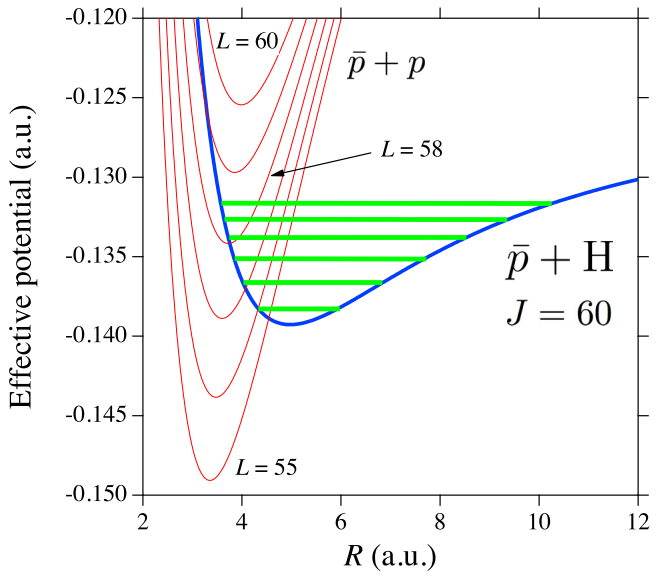

FIG. 14. Effective potentials relevant to the autodetachment $\bar{p}\mathrm{H}(v, J) \to \bar{p}p(N, L) + e$: $V_{\mathrm{eff}}(R) = J(J+1)/(2\mu R^2) + V_{100}(R)$ of $\bar{p}\mathrm{H}$ for $J = 60$, and $L(L+1)/(2\mu R^2) - 1/R$ of $\bar{p}p$ for $L =$ 55–60. The horizontal lines indicate the vibrational energy levels ($v =$ 0–5) of $\bar{p}\mathrm{H}(J = 60)$. For high v, the vibrational region overlaps the unstable area $R < R_0$.

can conclude that no autodetachment takes place for all the vibrational states ($0 \leqslant v < \infty$) of $\bar{p}\mathrm{H}$ if $65 \lesssim J \leqslant 73$.

Figure 10 shows that the predissociation is always negligible, and that the energy width is dominated by the autodetachment for low J and is dominated by the radiative dissociation for high J. The lifetime τ of $\bar{p}\mathrm{H}$ is defined by

$$\tau = \frac{1}{\Gamma_{\mathrm{dis}} + \Gamma_{\mathrm{rad}} + \Gamma_{\mathrm{det}}}, \tag{53}$$

and is shown for $\bar{p}\mathrm{H}(v = 0)$ in Fig. 15. For $J \geqslant 59$, the lifetime ($\sim 10^{-8}$ s) is essentially the radiative one. If the lifetimes were determined by only the spontaneous radiative emission, such species could be regarded as stable molecules. Thus, the $\bar{p}\mathrm{H}(v, J)$ species are stable molecules for all the vibrational states if $65 \lesssim J \leqslant 73$ and at least for a few lowest vibrational states if $59 \leqslant J < 65$. This is consistent with the finding obtained from the qualitative approach based on the detachment interaction range R_0 (Sec. III). If the stable $\bar{p}\mathrm{H}$ molecules were produced in experiments, several (v, J) states would be distributed. Then, as imagined from Fig. 11, the emitted photons would have continuum spectra that have a peak at the Ly-α position and a broad tail toward a low-energy side.

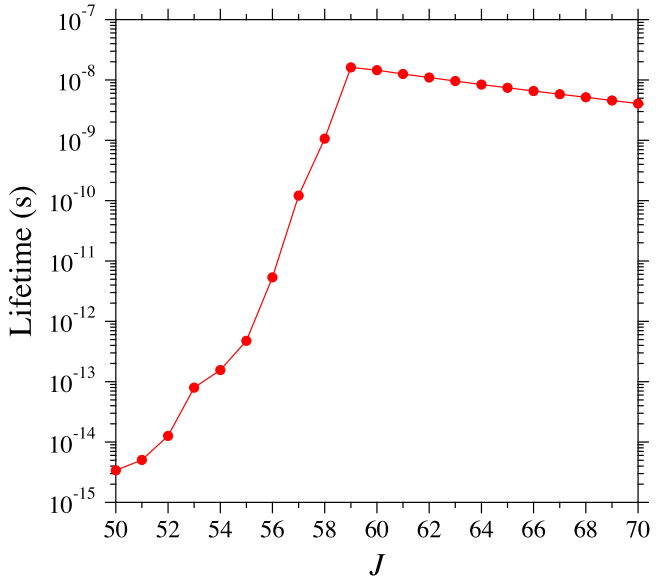

FIG. 15. Lifetimes of $\bar{p}\mathrm{H}(v = 0, J)$ for $J =$ 50–70.

VI. COMPARATIVE DISCUSSION

In this section, discussions are held by comparing $\bar{p}\mathrm{H}$ with hydrogen molecular ions $\mathrm{H_2}^+$ and $\mathrm{H_2}^-$. In some respects, the $\bar{p}\mathrm{H}$ system shows similarities to these molecular ions.

A. $\mathrm{H_2}^+$

The $p + \mathrm{H}$ and $\bar{p} + \mathrm{H}$ systems have the same mass combination, and their difference is only the opposite charge sign of p and $\bar{p}$. The $\mathrm{H_2}^+$ molecule in the electronic ground ($1s\sigma_{\mathrm{g}}$) state has no autoionization channel, and it is permanently stable. Due to the charge sign difference, the two systems are clearly distinct in the molecular stability. At large internuclear distances, however, the charge sign is irrelevant, and the $p + \mathrm{H}$ system exhibits the same electronic properties as those of $\bar{p} + \mathrm{H}$. Of the $\mathrm{H_2}^+$ potential curves that correlate with the separated atom $\mathrm{H}(n=2)$, the $2p\pi_{\mathrm{u}}$, $3d\sigma_{\mathrm{g}}$, and $4f\sigma_{\mathrm{u}}$ ones support vibrational levels [31,48]. The asymptotic state of $\bar{p}\mathrm{H}(1, 0, 0)$ is equivalent to the $\mathrm{H_2}^+(3d\sigma_{\mathrm{g}})$ and $\mathrm{H_2}^+(4f\sigma_{\mathrm{u}})$ states at large internuclear distances $R_{\mathrm{H_2}^+}$: The $3d\sigma_{\mathrm{g}}$ and $4f\sigma_{\mathrm{u}}$ potentials have the long-range attractive term $-3/R^2_{\mathrm{H_2}^+}$, and they support an infinite number of vibrational levels for any $J_{\mathrm{H_2}^+} \leqslant J_{\max}$ ($J_{\mathrm{H_2}^+}$ being the rotational quantum number of $\mathrm{H_2}^+$) [31]. Because of the same mass combination, $J_{\max} = 73$ is just the same as that for $\bar{p}\mathrm{H}(1, 0, 0)$. In this respect, the $\mathrm{H_2}^+(3d\sigma_{\mathrm{g}})$ and $\mathrm{H_2}^+(4f\sigma_{\mathrm{u}})$ molecules show an interesting similarity to $\bar{p}\mathrm{H}(1, 0, 0)$. The $\mathrm{H_2}^+(2s\sigma_{\mathrm{g}})$ and $\mathrm{H_2}^+(3p\sigma_{\mathrm{u}})$ states have the same asymptotic behavior as $\bar{p}\mathrm{H}(0, 1, 0)$, and they have the long-range repulsive term $+3/R^2_{\mathrm{H_2}^+}$ at large $R_{\mathrm{H_2}^+}$ [31]. The $\mathrm{H_2}^+(2p\pi_{\mathrm{u}})$ molecule corresponds to $\bar{p}\mathrm{H}(0, 0, \pm 1)$: The $2p\pi_{\mathrm{u}}$ potential has no long-range term $\propto \pm 1/R^2_{\mathrm{H_2}^+}$, and it can support only a finite number of vibrational levels [31].

One may expect that the experimental study of electronically excited $\mathrm{H_2}^+$ molecules is helpful for examining the creation of the $\bar{p}\mathrm{H}(1, 0, 0)$ molecules. So far, however, no direct spectroscopic measurements have been successfully performed for any electronic exited state of $\mathrm{H_2}^+$ [49]. A translational energy-loss study of $\mathrm{H_2}^+$, produced by electron impacts on $\mathrm{CH_4}$, confirmed the $2p\pi_{\mathrm{u}}$ state [50], but no experimental evidence was offered for the $3d\sigma_{\mathrm{g}}$ and $4f\sigma_{\mathrm{u}}$ states. The reason for the experimental difficulty is that, for example, the Franck-Condon factor is not large for the optically forbidden $1s\sigma_{\mathrm{g}}$-$3d\sigma_{\mathrm{g}}$ transition and is negligibly small for the optically allowed $1s\sigma_{\mathrm{g}}$-$4f\sigma_{\mathrm{u}}$ transition. (The positions of the potential minimum are $R_{\mathrm{H_2}^+} \simeq 8$ a.u. for $2p\pi_{\mathrm{u}}$, $R_{\mathrm{H_2}^+} \simeq$

9 a.u. for $3d\,\sigma_g$, and $R_{H_2^+} \simeq 21$ a.u. for $4f\,\sigma_u$, which are much greater than $R_{H_2^+} \simeq 2$ a.u. for $1s\,\sigma_g$ [48].) Even though the ground-state $H_2^+(1s\,\sigma_g)$ molecules are readily available, unfortunately the production and detection of $H_2^+(3d\,\sigma_g)$ and $H_2^+(4f\,\sigma_u)$ are not easy in experimental studies.

The vibrational levels of $H_2^+(2p\,\pi_u)$, $H_2^+(3d\,\sigma_g)$, and $H_2^+(4f\,\sigma_u)$ are far above the dissociation limit of $p + H(1s)$. Hence, the predissociation channel is open for these H_2^+ states. Nakashima *et al.* [51] carried out the quantum-chemistry calculation of $H_2^+(3d\,\sigma_g)$ including the nonadiabatic coupling, and they were thereby able to investigate the predissociation process. They found that the predissociation was negligible for $H_2^+(3d\,\sigma_g)$, as in the case of $\bar{p}H(1,0,0)$.

B. H_2^-

In a dynamical aspect, the five-body system of $H^- + H$ has a close similarity to $\bar{p} + H$. The electron cannot be bound at small internuclear distances $R_{H_2^-}$ in the electronic ground $(^2\Sigma_u^+)$ state, and the detachment promptly occurs in this system at $R_{H_2^-} \lesssim 3$ a.u. [52]. The feature of the $H_2^-(^2\Sigma_u^+)$ effective potentials is very similar to that shown in Fig. 2. The H_2^- molecule had been considered to be highly unstable due to autodetachment [53]. However, the existence of long-lived H_2^- species was confirmed by Golser *et al.* [54] using secondary-ion mass spectroscopy. In this experiment, the long-lived H_2^- species were produced by sputtering of TiH_2 targets with Cs^+ ion beams with an impact energy of ~5.4 keV. In theoretical studies, Čížek *et al.* [52,55] showed that this long-lived species could be $H_2^-(^2\Sigma_u^+)$ in a high angular momentum state with the vibrational energy above the dissociation limit, identified as a tunneling type of shape resonance. As in the case of $\bar{p}H$, with increasing the rotational quantum number $J_{H_2^-}$, the autodetachment of H_2^- is expected to become inhibited. The theoretical calculation provided the lifetime $\tau_{H_2^-} \sim 0.3\ \mu$s (controlled by the tunneling through the centrifugal barrier) for the resonance with $J_{H_2^-} = 26$ [55], while the experimental value was $\tau_{H_2^-} \simeq 8.2\ \mu$s for the long-lived species [56]. The reason for this discrepancy has not been explained in a precise sense [55].

Unfortunately, one cannot expect the existence of long-lived $\bar{p}H(0,0,0)$ species attributable to the tunneling type of shape resonance, which is dismissed in the present case of $\bar{p} + H(1s)$ collisions [25,57]. For the $H^- + H$ system with $J_{H_2^-} = 26$, the vibrational region of the resonance is located at $R_{H_2^-} > 3$ a.u. [55]. On the contrary, Fig. 2 shows that the vibrational regions are inside the detachment interaction range (~1.5 a.u.) for $\bar{p} + H(1s)$. This difference happens because the $H^- + H$ potential is much more attractive than the polarization potential at $4 \lesssim R_{H_2^-} \lesssim 10$ a.u. [58]. [The $\bar{p} + H(1s)$ potential is not largely different from the polarization potential at $R \gtrsim 4$ a.u.]

If the distance $R_{H_2^-}$ is very large, the H^- ion can be assumed to be a point charge when viewed from the H-atom side. Then, also for $H^- + H(n=2)$, the potential curve has asymptotically the long-range attractive term $(-3/R_{H_2^-}^2)$ (although no theoretical investigation has been done for such electronic states). In the same way as $\bar{p}H(1,0,0)$, the corresponding electronically excited H_2^- molecules with very high $J_{H_2^-}$ would be stable against autodetachment. In sputtering experiments using high-energy ion impacts, it would be possible to yield molecular products in electronic excited states. At the present time, the existence of long-lived H_2^- molecules in electronic excited states has not yet been confirmed in the experiments.

However, the sputtering experiment for H_2^- is suggestive. Indeed, chemical sputtering is available for producing various kinds of molecular species [59]. One may be able to expect that the experiments of the chemical sputtering of hydrogen-rich surfaces with $\bar{p}$ beams are useful for creating the $\bar{p}H(1,0,0)$ molecules.

VII. SUMMARY AND FURTHER DISCUSSION

The $\bar{p}H$ molecule in the electronic ground state $(n_1, n_2, \lambda) = (0,0,0)$ is always unstable. The present study shows that the stable $\bar{p}H$ molecule can exist if it is in the first electronic excited state $(n_1, n_2, \lambda) = (1,0,0)$. The $\bar{p}H(1,0,0)$ molecule has a notable decay channel of autodetachment that takes place at $R \lesssim 4$ a.u., and the vibrational motion reaching such a detachment region cannot be a stable state. Nonetheless, since the $\bar{p}H(1,0,0)$ molecule has asymptotically the long-range attractive potential $-3/R^2$, the stable high-J bound states can be realized: If J is very high, the vibrational motion remains far outside, and the autodetachment is suppressed. These high-J vibrational states can be reasonably described by the BO approximation. For the $\bar{p}H(1,0,0)$ molecule with $J \geqslant 59$, the autodetachment becomes negligible and the lifetime is dominated by the spontaneous radiative emission. If the angular momentum becomes $J \geqslant 74$, the $\bar{p}H(1,0,0)$ molecule is dissociated by a centrifugal force and cannot be stable. Although the $\bar{p}H(1,0,0)$ molecule has another decay channel of predissociation, it is always negligible.

It would be very interesting if the $\bar{p}H(1,0,0)$ molecules were created in elementary atomic and molecular processes. Over the course of the resonance collisions $\bar{p} + H(1s) \rightleftarrows \bar{p}H(1,0,0)$, the $\bar{p}H(1,0,0)$ species can be temporally formed. However, this would be unrealistic for creating the $\bar{p}H(1,0,0)$ molecules because the resonance width Γ_{dis} is quite small in the collisions. High-energy collisions of $\bar{p}$ with H_2^+ or H_2 may be a candidate process. Since the electronic excitation must be accompanied, the collision energy is necessarily $\gtrsim$keV. At such high energies, although the exchange chemical reaction is normally inefficient, equal-mass billiard-ball collisions between $\bar{p}$ and p may make it possible to produce the $\bar{p}H(1,0,0)$ molecules.

The long-range attractive interaction $\propto -1/R^2$ also works in $\bar{p} + H(n)$ with $n \geqslant 3$. Therefore, one can expect that stable $\bar{p}H$ molecules exist for high Rydberg states. The term $\propto 1/R^2$ in Eq. (10) is the most attractive for $(n_1, n_2, \lambda) = (n-1, 0, 0)$. In this case, the effective potential becomes attractive at large R if J satisfies

$$J < \left[3n(n-1)\mu - \frac{1}{4}\right]^{1/2} - \frac{1}{2}, \tag{54}$$

which becomes, for example, $J \leqslant 128$ for $n = 3$, $J \leqslant 181$ for $n = 4$, and $J \leqslant 234$ for $n = 5$. Since the radiative emission rate decreases rapidly with increasing n, the lifetime of the Rydberg $\bar{p}H$ molecule would become very long. The $\bar{p}H$

molecule having high n and very high J is expected to be quite stable. However, the nonadiabatic coupling becomes stronger for higher n, and hence the simple BO picture may not be appropriate for describing the Rydberg $\bar{p}$H molecular states. Exactly the same conclusion as in the present study can be derived also for the charge-conjugation system $p\bar{\mathrm{H}}$. In recent experimental studies of $\bar{\mathrm{H}}$ production [14–16], the $\bar{\mathrm{H}}$ atoms are cold and are found to be in high Rydberg states [60]. This suggests that the $p + \bar{\mathrm{H}}(n \geqslant 2)$ system rather than $\bar{p} + \mathrm{H}$ may be more favorable for realizing the creation of stable exotic molecules.

The three-body system of $\bar{p}$-p-e may have another type of resonance states ($\bar{p}p$-e): the dipole interaction between $\bar{p}p(N)$ and e can support the electron bound state at a total energy $E = E_N + \epsilon$ with $\epsilon < 0$ [31,37,61]. Unlike in the molecular state, the electron is not localized around the nucleus in this resonance. As $r \to \infty$, the centrifugal and dipole interactions for the electron can be expressed by

$$\frac{\mathbf{l}^2 + 2\hat{\mathbf{r}} \cdot \mathbf{R}}{2r^2}, \tag{55}$$

where $\mathbf{l}$ is the electron angular momentum operator. By diagonalizing the numerator with use of the degenerate states of $\bar{p}p(N)$, the effective potential for the electron becomes

$$V_{\mathrm{eff}}^{(e)}(r) \xrightarrow[r\to\infty]{} \frac{\Omega^{(e)}}{2r^2} + E_N. \tag{56}$$

The numerical calculation shows that the lowest eigenvalue becomes $\Omega^{(e)} < -1/4$ for $J \leqslant 26$ if $N = 30$ (corresponding to $E \sim -0.5$ a.u.), for $J \leqslant 48$ if $N = 50$ ($E \sim -0.2$ a.u.), and for $J \leqslant 69$ if $N = 70$ ($E \sim -0.1$ a.u.). In this case, the long-range tail in Eq. (56) can support an infinite number of bound states [33]. Unfortunately, no such resonances could be found at $E \sim -0.5$ a.u. in rigorous collision calculations [25,61]. Whether the resonance state supported by Eq. (56) can really exist at higher energies is an interesting subject. To examine this, a sophisticated calculation such as was done in Refs. [25,61] is necessary. However, such a calculation becomes much more troublesome at high energies, and it remains a goal of future work.

[1] C. J. Batty, Rep. Prog. Phys. **52**, 1165 (1989).
[2] E. Klempt, F. Bradamante, A. Martin, and J.-M. Richard, Phys. Rep. **368**, 119 (2002).
[3] D. B. Cassidy, T. H. Hisakado, H. W. K. Tom, and A. P. Mills, Jr., Phys. Rev. Lett. **108**, 043401 (2012).
[4] A. Rich, Rev. Mod. Phys. **53**, 127 (1981).
[5] J. Mitroy, M. W. J. Bromley, and G. G. Ryzhikh, J. Phys. B **35**, R81 (2002).
[6] Y. Nagashima, Phys. Rep. **545**, 95 (2014).
[7] D. B. Cassidy and A. P. Mills Jr., Nature (London) **449**, 195 (2007)
[8] D. Gotta, Prog. Part. Nucl. Phys. **52**, 133 (2004).
[9] T. Yamazaki, N. Morita, R. Hayano, E. Widmann, and J. Eades, Phys. Rep. **366**, 183 (2002).
[10] M. Hori, Phys. Rep. **403**, 337 (2004).
[11] R. S. Hayano, M. Hori, D. Horváth, and E. Widmann, Rep. Prog. Phys. **70**, 1995 (2007).
[12] M. Hori, H. Aghai-Khozani, A. Sótér, D. Barna, A. Dax, R. Hayano, T. Kobayashi, Y. Murakami, K. Todoroki, H. Yamada, D. Horváth, and L. Venturelli, Science **354**, 610 (2016).
[13] I. Shimamura, Phys. Rev. A **46**, 3776 (1992).
[14] N. Madsen, Philos. Trans. R. Soc. A **368**, 3671 (2010).
[15] W. A. Bertsche, E. Butler, M. Charlton, and N. Madsen, J. Phys. B **48**, 232001 (2015).
[16] M. Charlton, A. P. Mills Jr., and Y. Yamazaki, J. Phys. B **50**, 140201 (2017).
[17] B. R. Junker and J. N. Bardsley, Phys. Rev. Lett. **28**, 1227 (1972).
[18] W. Kolos, D. L. Morgan Jr., D. M. Schrader, and L. Wolniewicz, Phys. Rev. A **11**, 1792 (1975).
[19] B. Zygelman, A. Saenz, P. Froelich, S. Jonsell, and A. Dalgarno, Phys. Rev. A **63**, 052722 (2001).
[20] K. Strasburger, J. Phys. B **35**, L435 (2002).
[21] K. Strasburger, J. Phys. B **37**, 4483 (2004).
[22] B. Zygelman, A. Saenz, P. Froelich, and S. Jonsell, Phys. Rev. A **69**, 042715 (2004).
[23] P. Berggren, H. Stegeby, A. Voronin, and P. Froelich, J. Phys. B **41**, 155202 (2008).
[24] H. Stegeby and K. Piszczatowski, J. Phys. B **49**, 014002 (2016)
[25] K. Sakimoto, Phys. Rev. A **90**, 032514 (2014).
[26] E. Fermi and E. Teller, Phys. Rev. **72**, 399 (1947).
[27] A. S. Wightman, Phys. Rev. **77**, 521 (1950).
[28] J. E. Turner, Am. J. Phys. **45**, 758 (1977).
[29] R. F. Wallis, R. Herman, and H. W. Milnes, J. Mol. Spectrosc. **4**, 51 (1960).
[30] K. Sakimoto, Phys. Rev. A **65**, 012706 (2001).
[31] I. Shimamura, Phys. Rev. A **40**, 4863 (1989).
[32] K. Sakimoto, Eur. Phys. J. D **72**, 17 (2018).
[33] L. D. Landau and E. M. Lifshitz, *Quantum Mechanics*, 3rd ed. (Pergamon, Oxford, 1977).
[34] M. Kotani, K. Ohno, and K. Kayama, *Quantum Mechanics of Electronic Structure of Simple Molecules, Handbuch der Physik XXXVII/2* (Springer-Verlag, Berlin, 1961).
[35] C. A. Coulson and M. Walmsley, Proc. Phys. Soc. **91**, 31 (1967).
[36] O. H. Crawford, Proc. Phys. Soc. **91**, 279 (1967).
[37] M. J. Seaton, Proc. Phys. Soc. **77**, 174 (1961).
[38] J. S. Cohen, R. L. Martin, and W. R. Wadt, Phys. Rev. A **24**, 33 (1981).
[39] P. R. Žďánská, H. R. Sadeghpour, and N. Moiseyev, J. Phys. B **37**, L35 (2004).
[40] D. Baye and P.-H. Heenen, J. Phys. A **19**, 2041 (1986).
[41] K. Sakimoto, J. Phys. B **33**, 5165 (2000).
[42] N. F. Mott and H. S. W. Massey, *Theory of Atomic Collisions*, 3rd. ed. (Claendon, Oxford, 1965), p. 357.
[43] T. L. Stephens and A. Dalgarno, J. Quant. Spectrosc. Radiat. Transf. **12**, 569 (1972).
[44] R. Ahlrichs, O. Dumbrajs, H. Pilkuhn, and H. G. Schlaile, Z. Phys. A **306**, 297 (1982).
[45] V. I. Korobov and I. Shimamura, Phys. Rev. A **56**, 4587 (1997).

[46] K. Sakimoto, Phys. Rev. A **84**, 032501 (2011).
[47] B. H. Choi and R. T. Poe, Phys. Rev. A **16**, 1821 (1977).
[48] M. M. Madison and J. M. Peek, At. Data Nucl. Data Tables **2**, 171 (1971).
[49] A. Carrington, I. R. McNab, and C. A. Montgomerie, J. Phys. B **22**, 3551 (1989).
[50] N. J. Kirchner, A. O'Keefe, J. R. Gilbert, and M. T. Bowers, Phys. Rev. Lett. **52**, 26 (1984).
[51] H. Nakashima, Y. Hijikata, and H. Nakatsuji, Astrophys. J. **770**, 144 (2013).
[52] M. Čížek, J. Horáček, and W. Domcke, J. Phys. B **31**, 2571 (1998).
[53] J. Horáček, M. Čížek, K. Houfek, and P. Kolorenč, in *Proceedings of the 5th International Conference on Atomic and Molecular Data and Their Applications (ICAMDATA)*, AIP Conference Proceedings No. 901, edited by E. Roueff (AIP, New York, 2007), p. 147.
[54] R. Golser, H. Gnaser, W. Kutschera, A. Priller, P. Steier, A. Wallner, M. Čížek, J. Horáček, and W. Domcke, Phys. Rev. Lett. **94**, 223003 (2005).
[55] M. Čížek, J. Horáček, and W. Domcke, Phys. Rev. A **75**, 012507 (2007).
[56] O. Heber, R. Golser, H. Gnaser, D. Berkovits, Y. Toker, M. Eritt, M. L. Rappaport, and D. Zajfman, Phys. Rev. A **73**, 060501 (2006).
[57] K. Sakimoto, Phys. Rev. A **94**, 042701 (2016).
[58] L. Senekowitsch, P. Rosmus, W. Domcke, and H.-J. Werner, Chem. Phys. Lett. **111**, 211 (1984).
[59] V. Grill, J. Shen, C. Evans, and R. G. Cooks, Rev. Sci. Instrum. **72**, 3149 (2001).
[60] G. Gabrielse, N. S. Bowden, P. Oxley, A. Speck, C. H. Storry, J. N. Tan, M. Wessels, D. Grzonka, W. Oelert, G. Schepers, T. Sefzick, J. Walz, H. Pittner, T. W. Hänsch, and E. A. Hessels, Phys. Rev. Lett. **89**, 213401 (2002).
[61] K. Sakimoto, Phys. Rev. A **78**, 042509 (2008).